



The Impulse Pattern Formulation (IPF) as a nonlinear model of musical instruments

Simon LINKE^(1,2), Rolf BADER⁽¹⁾, Robert MORES⁽²⁾,

⁽¹⁾Institute of Systematic Musicology, University of Hamburg Germany

⁽²⁾Hamburg University of Applied Sciences, Germany*

Abstract

The Impulse Pattern Formulation (IPF) is a top-down method which assumes musical instruments to work with impulses which are produced at a generator, travel through the instrument, are reflected at various positions, are exponentially damped and finally trigger or at least interact with succeeding impulses produced by the generator. The underlying recursive equation relates every new system state to previous values and their logarithm. Adding more system components increases the number of reflection points, thus the number of terms in the argument of the logarithmic function increases. Like other nonlinear equations, the IPF can produce stable states but also bifurcation and divergency and fully captures transitions between regular periodicity at nominal pitch, bifurcation scenarios, and noise.

Applying the IPF on musical Instruments, the nonlinear behavior like transients or multiphonics can be described, which would be very complicated or impossible using well-established methods such as modal analysis or finite element models. Furthermore, the IPF is used for sound synthesis which follows the fundamental principles of real musical instruments and, due to the simple mathematical description of the IPF, needs a very limited number of input parameters.

Keywords: Analysis, Modelling, Musical Instruments, Nonlinearities, Synthesis

1 INTRODUCTION

Understanding the fundamental principles of musical instruments has always been a crucial question in Musicology. As musical instruments in general consist of many somehow coupled components, there is a demand for simple model systems. Basic, linear models derived from mechanics or electro-dynamics yield to satisfying results when describing more general phenomenon, but they are lacking experimental evidence when dealing with real instruments. As Fletcher [9] states it is not possible to explain the perfect harmonic spectrum of sustained instruments without taking nonlinearity into account. Further, there are more sophisticated approaches like physical modelling. They offer decent answers even for very detailed questions, but they can be hardly transferred to other problems and usually need lots of calculations.

The Impulse Pattern Formulation (IPF) is a top-down model, which describes systems in the time domain in a strictly nonlinear manner. Due to its very general approach the IPF can be used to observe any arbitrary system which consists of mutually coupled subsystems concerning its stability and is able to reproduce complex transient behavior. Thus, the IPF can be transferred to any arbitrary instrument and further has the potential to be extended to completely different disciplines like neuroscience or network theory.

The following work gives a short overview of the IPF according to [4]. Further, some basic analytical considerations are carried out, to explore mathematical boundaries of the IPF which are necessary to apply the IPF to real systems. Finally, in sections 3 to 5 three different systems are observed to illustrate how the required modeling parameters are chosen and how the results can be interpreted.

*simon.linke@haw-hamburg.de

2 MATHEMATICAL DESCRIPTION

2.1 Derivation

According to Bader [5] musical instruments in general should be considered as self-organized systems. Particularly he assumes every instrument to be driven by impulses. This is reasonable for percussion or plucked string instruments, but it is also plausible for any other instrument, for instance reed and brass instruments: The valve-like behavior of the reed, or the lips of the player leads to distinguished single impulses entering the tube. Musical instruments are often described as a generator acting on a resonator (e.g. [10]). The IPF is somewhat more general: A musical instrument is a system acting upon itself, consisting of mutually coupled subsystems, possibly even interacting backwards. The system can be analyzed from the perspective of any subsystem, as it sends out impulses while responding to other subsystems. To make this a little bit more ostensive, we choose the simple example of a reed instrument e.g. a saxophone. It consists of two subsystems: a reed and a tube. Taking the point of view on the reed, the reed sends out impulses which are answered by the tube. According to Bader [4, p. 286] the answer is just a callback of the impulses send out by the reed. As the back-traveling impulses have an impact on the reed, the change of the system is caused by the system itself:

$$\frac{\partial \bar{g}}{\partial t} = \frac{1}{\alpha} \bar{g} \quad (1)$$

where α is the strength of the back-traveling impulse. In the chosen example of a reed instrument, this is related to the playing pressure. The system state is represented by \bar{g} . Bader [4, p. 286] states that it is connected to the amplitude and the periodicity of a signal. The meaning depends on the system which is observed. In the sections 3, 4 and 5 is meaning of g for three different musical instruments discussed.

According to physics it must be assumed that the impulse needs a certain amount of time to travel through the tube and back to the reed. Furthermore, the impulse would be exponentially damped. Thus, Bader [4, pp. 286-288] deduces the IPF in its most simple form:

$$g_+ = g - \ln\left(\frac{g}{\alpha}\right) \quad (2)$$

Where g is the system state for a given time step and g_+ is the system state for the following time step. There is no precise time interval between g and g_+ . It is just the time until a new event occurs. Usually, this is just one fundamental period $T = 1/f$. Choosing an initial value g_0 , Equation (2) can be iteratively calculated. Observing the limits of the resulting sequence, it can be shown that the IPF can diverge or converge to a limit, depending on α . Furthermore, the IPF can show chaotic behavior like bifurcations. The limits for the IPF depending on α are shown in Figure 1. Bader [4, pp. 294] showed that for a constant control parameter α the IPF usually converge after $n > 300$ iteration steps. Therefore, 2500 iteration steps of Equation (2) were performed. To distinguish between bifurcations and chaotic behavior, the last 500 values g_n were taken into account.

Comparing Figure 1 with the chosen example of a reed instrument, we get a raw impression of the tone production: Low playing pressure, resulting in high values $1/\alpha$, is represented on the right side of the chart. The shown unstable behavior results in noisy sounds. Increasing the playing pressure α results in bifurcations. Here multiple frequencies can be heard at the same time. Further increasing of the pressure leads to stable states resulting in regular periodic motion.

By now, systems consisting of only two subsystems were described. Adding more subsystems results in adding more reflection points. Thus, the send-out impulse will return at additional (later) time steps, with individual strength β_k . Hence, the system state of earlier time points g_{k-} gains influence on the new system state g_+ . According to these assumptions, Bader [4, pp. 290-291] describes the IPF in its most general form:

$$g_+ = g - \ln\left(\frac{1}{\alpha} \left(g - \sum_{k=1}^n \beta_k e^{g - g_{k-}}\right)\right) \quad (3)$$

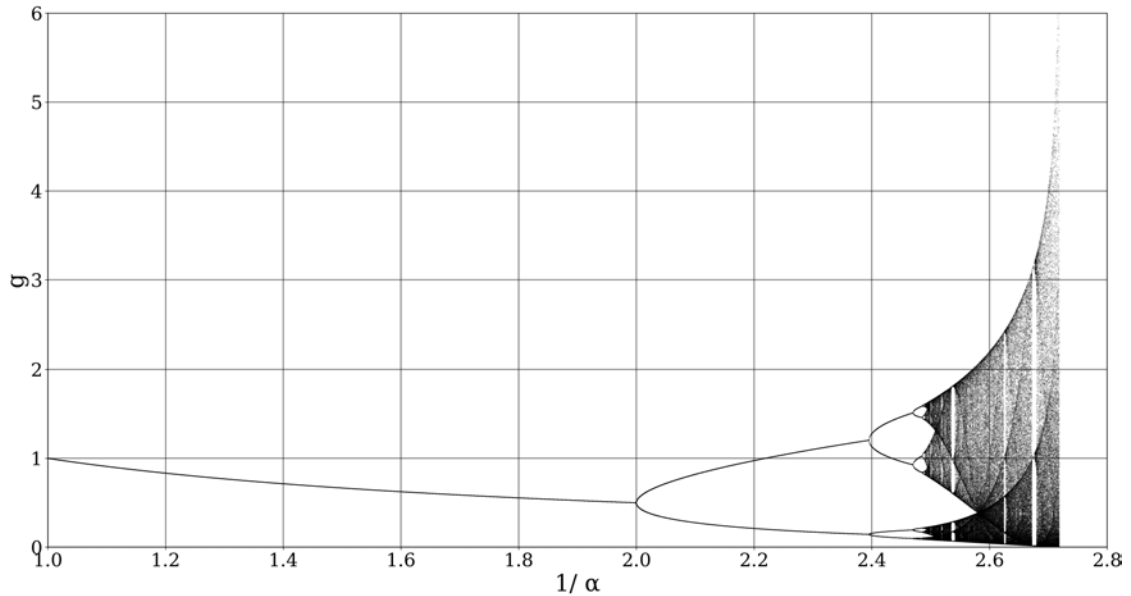


Figure 1. Bifurcation scenario of the IPF with one reflection point

Depending on β_k the IPF can become quite complex. The bifurcation scenario can be similar to the one described in Figure 1. But adding just one single reflection point, can change this significantly. Figure 2 shows the bifurcation scenario for a single reflection point $\beta = 0.164$. Due to the exponential function in Equation (3) two initial values g_{01} and g_{02} must be assumed. When choosing $g_{01} = 0.3$ and $g_{02} = 0$ there is no straight transition from stable, via chaotic to diverging states, directly. It is possible to return from a chaotic stage back to a stable state. Also, stable and chaotic domains can be interrupted by small diverging regions.

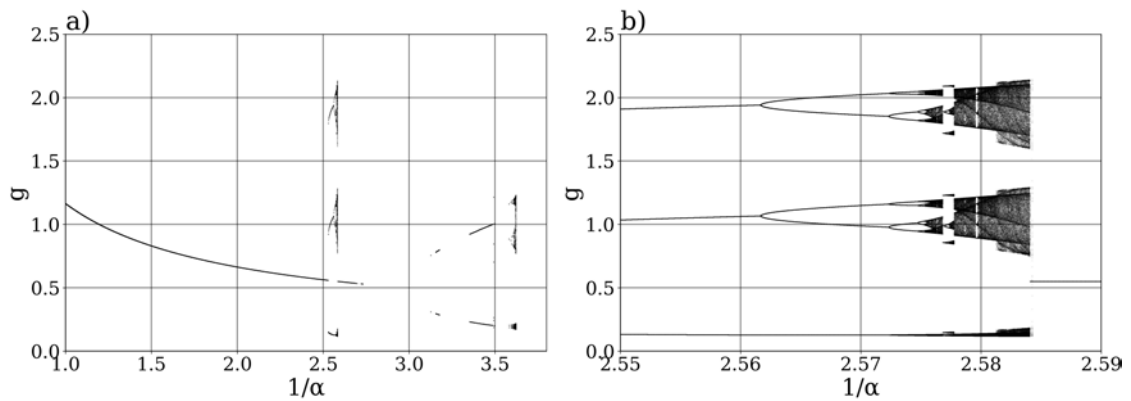


Figure 2. Bifurcation scenario of the IPF with two reflection points in dependence of $1/\alpha$ with $\beta = 0.164$. The right chart b) is a zoom of the chaotic region.

2.2 Boundaries and Stability

Referring to Bader [4, pp. 286-288] the parameter α is the input strength of the system. Therefore, only positive values α are physically reasonable. As β_k are the reflection strengths they had to be positive, too. If

the conservation of energy is valid, the following restriction can be derived:

$$\alpha \geq \sum_{k=1}^n \beta_k \tag{4}$$

According to Bader [4, p. 291], higher orders k will result in smaller β_k , as they represent reflection points farther away from the excitation point. Therefore, reflected impulses return later and weaker. Hence, there is a second condition for the relationship of α and β_k :

$$\alpha > \beta_1 > \beta_2 > \beta_3 > \dots > \beta_n \tag{5}$$

Referring to Figure 1, parameter g reaches no values above $1/\alpha \approx 2.7$. In this region g becomes complex and starts to diverge. Consequently, there seems to be a minimum α_{min} , which is the lower boundary for physically reasonable behavior. The only possibility to get complex values g_+ is, if the argument of the logarithm in Equation (3) is negative. Focusing on the simplest case with only one reflection point ($\beta_k = 0 \forall k$), $g \leq 0$ must be valid. As the IPF is a recursive formula, this can be achieved, once the right-hand side (rhs) of Equation (2) is equal to zero. Thus, the critical value α_{min} must be described as a function in dependence of g :

$$\alpha_{min} = \frac{g}{e^g} \tag{6}$$

To find an expression of α_{min} , which is true for any g , the global maximum of function (6) must be calculated. Determining the first and second derivative results in one single maximum at $g = 1$, which also accords with the previous observation of Figure 1.:

$$\frac{1}{\alpha_{min}} = e \approx 2.7 \tag{7}$$

This approach could be expanded, to determine α_{min} for systems with more than one reflection point. But then, the expression depends on the different reflection strengths β_k and according to Equation (3) to the previous system states g_{k-} . Thus, the equation depends on the initial value g_0 and an analytical solution is no longer possible.

There is a fixed point $f(g_s) = g_s$ of the IPF, where the system state g is constant for all time points:

$$g_- = g = g_+ = g_{2+} = \dots = g_{n+} = g_s \tag{8}$$

Thus, simplifying Equation (3) leads to a fixed point:

$$g_s = g_s - \ln \left(\frac{1}{\alpha} \left(g_s - \sum_{k=1}^n \beta_k e^{g_s - g_s} \right) \right)$$

$$g_s = \alpha + \sum_{k=1}^n \beta_k \tag{9}$$

A fixed point g_s exists for any combination of α and β_n , but according to Argyris et al. [1, pp.65-66] it is only stable if the absolute value of the first derivative is lower than 1. As the derivative depends again on the previous values g_{k-} and therefore on g_0 an analytic solution could be determined only for systems with one single reflection point ($\beta_k = 0 \forall k$):

$$|f'(g_s)| = \left| 1 - \frac{1}{\alpha} \right| < 1$$

$$\alpha > 0.5 \tag{10}$$

The critical point $\alpha_c = 0.5$ is called the first bifurcation point. If $\alpha > \alpha_c$ there exists only one stable fixed point. If α is lower than 0.5 bifurcations occur. Further decreasing of α leads to bifurcation of higher orders. This behavior can be easily verified when looking at Figure 1.

3 THE DIZI-FLUTE

Mirlitons are a special case of wind instruments. Here, one of the holes is equipped with a thin membrane [4, p. 227]. A representative of those instruments is the Dizi, a traditional Chinese transverse flute. It consists of bamboo and in contrast to traditional European transverse flutes there is an additional hole with a mirliton membrane attached, between the blowing hole and the first finger hole [18]. The sound is described to be nasal and buzzing [2], but also to be rough and rich in odd upper partials which result in multi-pitch effects [19].

Bader [4, pp. 227-228] compared two different dizi sounds of the same fundamental pitch. But while one sound was recorded playing the dizi how it is supposed to be, the second sound was recorded with a finger covering the membrane hole, to estimate its influence. He deduces that the membrane adds a noticeable amount of roughness to the sound and even though the overall spectrum stays harmonic each partial gets surrounded by sidebands. The resulting spectrum shown in Figure 3 a) also shows an increasing amount of higher partials.

Such an behavior could be explained by frequency modulation (FM) according to Chowning [6], where a modulating frequency which correspond to the fundamental frequency f_0 extends the spectrum to higher partials and a second significantly lower modulating frequency is responsible for the sidebands of each partials. These two modulation frequencies could be condensed to one modulating frequency fluctuating around f_0 . There had already been some approaches to model the dizi using FM (e.g. [2]) but they rather focusing on the transition between to tones, than on the influence of the membrane hole. When modelling the dizi using the IPF the

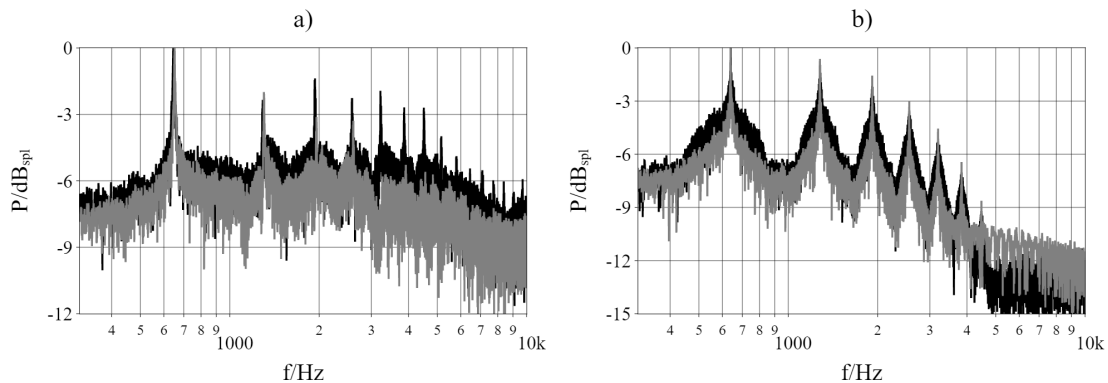


Figure 3. Spectrum of the dizi with (black) and without (gray) a mirliton membrane attached. Where a) corresponds to a measurement and b) to a model using the IPF

necessary number of β_k must be derived from the instrument geometry. If the membrane hole is covered, only one reflection point exists. An impulse entering at the embouchure gets reflected at the first open finger hole (or end of the tube, if all finger holes are closed) and returns to the embouchure. Thus, only α and no β_k is necessary to describe the resulting behavior. Releasing the finger from the membrane hole, adds an additional reflection points and thus β_1 .

As α is related to the blowing pressure, it changes during tone production. To obtain a realistic time series of α , the envelope of a recorded dizi sound is chosen. Then a suitable normalization is necessary. The IPF should not diverge but preferably all possible values of α should be utilized. As the membrane hole is closed alpha can be normalized to the interval $[1/e, 1]$ according to Equation (7). If the membrane hole is opened, a suitable value α_{min} in accordance to the chose β_1 must be determined numerically.

With Equation (3) a time series of different g can be calculated using α . Just by observing this time series it is possible to deduce if stable or instable tones are produced. Further, focusing on the transition from instable to stable states, the transient behavior of the dizi can be determined. But for sound production the underlying waveform must be estimated. The spectral content of the waveform is crucial for the produced sound. To

stay close to the motivation of the IPF a sharp Gaussian function is chosen. Thus, the resulting sound can be archived, just by creating a train of those Gaussian pulses. But the length of every pulse must be modulated in respect to the change of g . The resulting period-length T_k could be described as:

$$T_k = \frac{1}{f_0} (1 + (g_k - g_{k-})) \quad (11)$$

where g_k is the current and g_{k-} is the previous system state. If the system is stable every system state corresponds to the fixed point $g_k = g_{k-} = g_s$. Thus, results in a tone with the fundamental frequency f_0 . Bifurcations or transient behavior are leading to a frequency simulation similar as described above. According to Bader [4, p. 286] g is also connected to the amplitude. Thus, every Gaussian pulse is weighted by the actual system state g_k . The resulting sound equals the spectral properties of the dizi, but for a more realistic envelope, the resulting signal could be multiplied with the blowing pressure α .

The modelled sounds, as well as the recordings of the dizi, are provided by [12]¹. It is notable, that there is a strong evidence in the change of the sound when adding β_k respectively a mirliton membrane. Still there are some remarkable differences between the model and the recording, as the underlying equation and waveform have been chosen as simple as possible. Looking at the two different spectra in Figure 3 b), it is glaring that adding $\beta_1 = 0.245$ leads to sidebands. Although there is less influence of higher partials, the model in general corresponds to the behavior of a dizi with and without membrane.

4 MULTIPHONICS IN REED INSTRUMENTS

In reed instruments there are several technics to produce sounds with more than one harmonic overtone spectrum [4, p. 226]. One common way to produce these so-called multiphonics is the use of uncommon fingerings [3]. For stable tone production the first open hole determines the length of the tube and thus the fundamental frequency. Up to the first open hole all holes are closed and further down all holes are open. When producing multiphonics more complex patterns of open and closed holes are used. Further, the embouchure and the (usually low) blowing pressure must be controlled very carefully [4].

Figure 4 shows a fingering for an multiphonic played on a clarinet, which can be found in multiple collection of multiphonic fingerings (e.g. [16] and [8]). The resulting sound is described to consist of two dominating frequencies which approximately could be notated as the musical interval E_4-G_5 . There are three regions of open holes which are likely to reflect the sound wave propagating through the tube. Those can be transferred to the IPF. The first reflection point occurs due to the open register key on the back. It lies closely under the barrel-joint and is represented by α . The press C#-key results in another open hole on the back of the instruments. It lies close to the open hole in the middle of the instruments. So, both could be condensed to one reflection point β_1 . The end of the tube is caused by two open holes between the undermost key and the bell and is represented by β_2 .

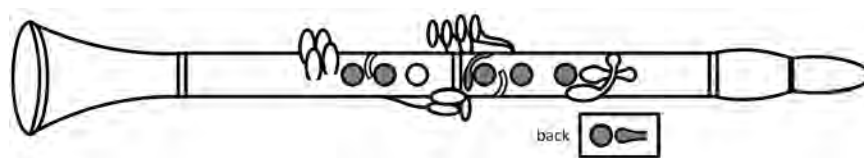


Figure 4. Sketch of a Clarinet: Grey circles correspond to closed holes when producing the investigated multiphonic.

When modeling multiphonics using the IPF, it is plausible that they are related to bifurcating regions. Here, the audible intervals are represented by the ratio of the possible system states g_k/g_{k-} . Thus, it can be examined

¹<https://zenodo.org/record/3258207#.XSSd8Y9CQuU>

numerically, which combinations of β_1 and β_2 are able to produce the given interval of 15 semitones for any initial value g_0 . As this is possible for many combinations, it is assumed that for reliable production of multiphonics small changes of blowing pressure or embouchure should not change the sound excessively. Therefore the derivative of g_k/g_{k-} in respect to α should be as small as possible. For the given multiphonic this could be achieved choosing $\beta_1 \approx 2.5 \cdot 10^{-3}$ and $\beta_2 \approx 0.35$. Where it is conspicuous that this violates condition (5).

Choosing an appropriate time series for α sounds can be synthesized in a similar manner as already done in section 3. Again, a Gaussian pulse is chosen as a raw approximation of the fundamental waveform. But this time it must be modulated slightly differently, according to the different interpretation of g mentioned above. The length of every period t is changed according to the ratio of the system states:

$$T = \frac{1}{f_0} \frac{g}{\tilde{g}} \quad (12)$$

where g is the actual system state. Choosing $\tilde{g} = g$ results in a signal that oscillates with the fundamental frequency f_0 . Now a second signal can be added, where \tilde{g} equals the previous system state g_- . Thus, both signals oscillate with the same frequency f_0 if $g = g_- = g_S$. As soon as bifurcation occurs, two pitches are perceived. Adding additional signals where \tilde{g} equals earlier system states ($g_{2-}, g_{3-}, g_{4-}, \dots$) allows to synthesize bifurcations of higher order.

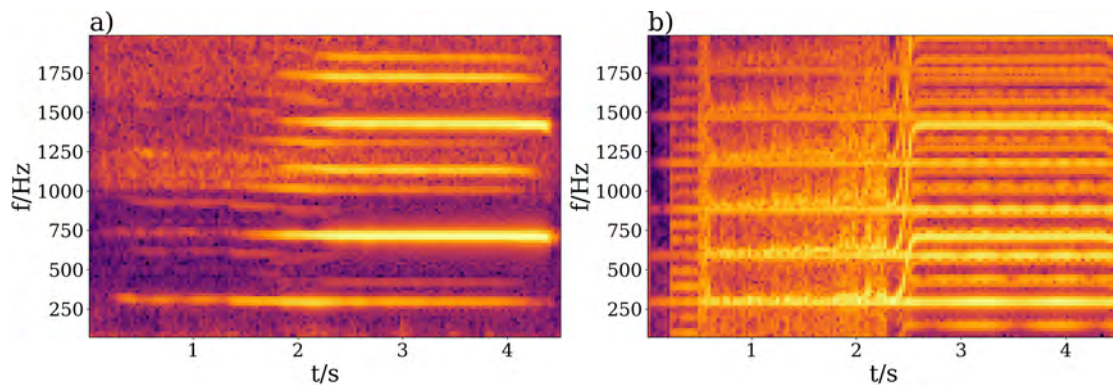


Figure 5. Spectrogram of a) a recorded multiphonic and b) its synthesized version

The multiphonic sound mentioned above was recorded. Slowly adjusting embouchure and blowing pressure allows a transition from a stable sound to a bifurcation. Comparing this sound with a synthesized version (both provided by [12]²) shows that both present a sudden transition from one to two pitches and no remarkable pitch glide, even though α was gradually changed. Figure 5 shows the related spectrograms. Looking at the synthesized version b) a pitch glide can be noticed but only during a very short period of time. Further, it is obvious that a Gaussian pulse as the fundamental waveform was not the ideal choice, as there is a strong spectral difference between the model and the recording even for stable tones with one perceived pitch.

5 THE BOWED STRING

The motion of a bowed string has always been a much-discussed question [10]. While bowing, the bow displaces the string due to the stickiness of the rosin. As the restoring force of the string exceeds the static friction of the bow, the string suddenly slips back. Subsequently the bow recaptures the string again, resulting in periodic motion of the string called Helmholtz motion [11]. But such behavior only occurs if the right ratio of bow

²<https://zenodo.org/record/3258207#.XSSd8Y9CQuU>

force F and bow velocity v_b (in respect to the bowing position) is applied. If the bow force is low, the strings slips back to early and gets recaptured by the bow before reaching the equilibrium. Those effects can emerge several times during one period T and result in frequency doubling and scratchy sounds [7, p.58]. Several attempts have been made to find an analytical expression for the necessary minimum bow force (e.g. first time by Raman [15] in 1918 and most prominent by Schelleng [17]). Mores [14] showed, that those expressions change drastically when treating the bow-string interaction as a self-organized system. Further, the transition time from unstable to Helmholtz motion is crucial for quality of bowed string instruments, as Giordano [11] stated. Since the IPF (due to its recursive formulation) is a straightforward model of transient behavior, it seems to be an appropriated solution for investigating this transition. Thus, a dynamical model of the complex transient behavior of a bowed string is obtained, rather than an analytical expression for a quasi-stationary minimum bow force.

The bow-string interaction of a monochord is measured using and a self-organized bowing pendulum as described by [13]. Transition from unstable to Helmholtz motion are achieved by slowly increasing the bow force. When just focusing on bow-string interaction and neglecting all other instrument parts the system can be described by the IPF in its most simple form as given by Equation (2). Then a suitable time series of α is assumed to model the measurement. Thus, an analytical expression for α in respect to bow force and bow velocity could be determined in future research.

As underlying waveform one period of the measured Helmholtz motion is chosen. Again, the amplitude of each period is multiplied with the actual system state g . Another sawtooth signal (with lower amplitude) is added, but every period is phase-shifted proportional to $g - g_-$. Thus, double slips can occur during transients or bifurcations. Two more sawtooth signals are added with phase-shifts proportional to $g - g_{2-}$ and $g - g_{3-}$, to achieve more realistic transients. The amplitudes of added signals are decaying according to the harmonic series. The number of added sawtooth signals as well the decaying of their amplitudes refers to the assumed dampening of the string.

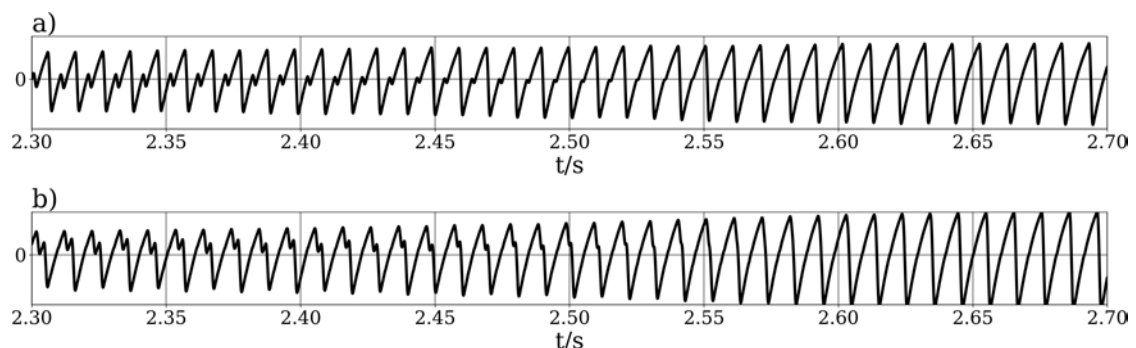


Figure 6. Timeseries of the transition into Helmholtz motion for measured (above) and modeled bow-string interaction (below)

Figure 6 compares the transition into Helmholtz motion of a measured bow-string interaction to the modeled transition. The general behavior is again similar, but the amplitude of the double-slip seems to be too large. They sound very similar too, but it is conspicuous, that when double slips occur, subharmonics are dominating in the synthesized sound, while in the recorded version the upper partials are prominent. This can be perceived when listening to both sounds, as they are provided by [12]³. This can be avoided if the ratio between amplitude modulation and the introduced phase shift is balanced more carefully.

³<https://zenodo.org/record/3258207#.XSSd8Y9CQuU>

6 CONCLUSIONS

The IPF as introduced in section 2 can model a variety of musical instruments. Only a very limited amount of system parameters (α and β_k) must be deduced when making reliable observations concerning the system stability. For an elaborated investigation of the produced sound, a suitable interpretation of g is crucial. Therefore, some deeper knowledge about the fundamental principles of the observed system is necessary. Three different interpretations of g were given in the sections 3 to 5. In addition, the fundamental spectral content must be chosen very carefully, if the IPF is supposed to be used as a synthesizer.

In future research a deeper comparison between the chosen set of modeling-parameters and measurements of real instruments should be done. Hence, it would be possible to deduce for instance an appropriated set of β_k just from measurements of the instrument geometry or physical input parameter like blowing pressure or bow force could be analytically map to α . Thus, some more profound observations concerning the system stability would be possible.

REFERENCES

- [1] J. H. Argyris, G. Faust, M. Haase, and R. Friedrich. *An Exploration of Dynamical Systems and Chaos: Completely Revised and Enlarged Second Edition*. Springer Berlin Heidelberg, Berlin, Heidelberg, 2015.
- [2] L. Ayers. Synthesizing trills for the chinese dizi. In *ICMC*, 2003.
- [3] J. Backus. Multiphonic tones in the woodwind instruments. *The Journal of the Acoustical Society of America*, 63(2):591–599, 1978.
- [4] R. Bader. *Nonlinearities and synchronization in musical acoustics and music psychology*, volume 2 of *Current research in systematic musicology*. Springer, Berlin [et al.], 2013.
- [5] R. Bader, editor. *Sound - Perception - Performance*, volume 1 of *Current research in systematic musicology*. Springer, Heidelberg, 2013.
- [6] J. M. Chowning. The synthesis of complex audio spectra by means of frequency modulation. *Journal of the Audio Engineering Society*, 21(7):526–534, 1973.
- [7] L. Cremer. *Physik der Geige*. Hirzel, Stuttgart, 1981.
- [8] G. J. Farmer. *Multiphonic trills and tremolos for clarinet*. PhD thesis, @Eugene, Or., Univ. of Oregon, Diss., Ann Arbor, Mich., 1977.
- [9] N. H. Fletcher. Mode locking in nonlinearly excited inharmonic musical oscillators. *The Journal of the Acoustical Society of America*, 64(6):1566–1569, 1978.
- [10] N. H. Fletcher and T. D. Rossing. *The physics of musical instruments*. Springer, New York, NY, 2. ed., [rpt.] edition, 2010.
- [11] N. Giordano. Some observations on the physics of stringed instruments. In R. Bader, editor, *Springer Handbook of Systematic Musicology*, Springer Handbooks, pages 105–119. Springer, Berlin, Heidelberg, 2018.
- [12] S. Linke. Sounds, synthesized using impulse pattern formulation, 2019.
- [13] R. Mores. Precise cello bowing pendulum. *Proc. of the Third Vienna Talk on Music Acoustics*, 106, 2015.
- [14] R. Mores. Complementary empirical data on minimum bow force. *The Journal of the Acoustical Society of America*, 142(2):728–736, 2017.

- [15] C. V. Raman. On the mechanical theory of the vibrations of bowed strings and of musical instruments of the violin family, with experimental verification of the results: Part 1. *Indian Assoc. Cultiv. Sci. Bull.*, 15:1–158, 1918.
- [16] H. Roche. 27 easy bb clarinet multiphonics, 2018.
- [17] J. C. Schelleng. The bowed string and the player. *The Journal of the Acoustical Society of America*, 53(1):26–41, 1973.
- [18] A. Thrasher. The transverse flute in traditional chinese music. *Asian Music*, 10(1):92, 1978.
- [19] C.-G. Tsai. The timbre space of the chinese membrane flute (dizi): Physical basis and psychoacoustical effects. *The Journal of the Acoustical Society of America*, 116(4):2620, 2004.